analytical chemistry

Article

pubs.acs.org/ac

Reproducible Automated Phosphopeptide Enrichment Using Magnetic TiO_2 and Ti-IMAC

Christopher J. Tape,[†,‡] Jonathan D. Worboys,[†] John Sinclair,[†] Robert Gourlay,[§] Janis Vogt,[§] Kelly M. McMahon,[∥] Matthias Trost,[§] Douglas A. Lauffenburger,[‡] Douglas J. Lamont,[§] and Claus Jørgensen*[,†,∥]

[†]The Institute of Cancer Research, 237 Fulham Road, London SW3 6JB, United Kingdom

[‡]Department of Biological Engineering, Massachusetts Institute of Technology, Cambridge, Massachusetts 02139, United States

[§]FingerPrints Proteomics Facility, College of Life Sciences, University of Dundee, Dundee DD1 5EH, United Kingdom

[∥]Cancer Research UK Manchester Institute, The University of Manchester, Wilmslow Road, Manchester M20 4BX, United Kingdom

Supporting Information

ABSTRACT: Reproducible, comprehensive phosphopeptide enrichment is essential for studying phosphorylation-regulated processes. Here, we describe the application of hyper-porous magnetic TiO_2 and Ti-IMAC microspheres for uniform automated phosphopeptide enrichment. Combining magnetic microspheres with a magnetic particle-handling robot enables rapid (45 min), reproducible ($r2 \geq 0.80$) and high-fidelity (>90% purity) phosphopeptide purification in a 96-well format. Automated phosphopeptide enrichment demonstrates reproducible synthetic phosphopeptide recovery across 2 orders of magnitude, "well-to-well" quantitative reproducibility indistinguishable to internal SILAC standards, and robust "plate-to-plate" reproducibility across 5 days of independent enrichments. As a result, automated phosphopeptide enrichment enables statistical analysis of label-free phosphoproteomic samples in a high-throughput manner. This technique uses commercially available, off-the-shelf components and can be easily adopted by any laboratory interested in phosphoproteomic analysis. We provide a free downloadable automated phosphopeptide enrichment program to facilitate uniform interlaboratory collaboration and exchange of phosphoproteomic data sets.

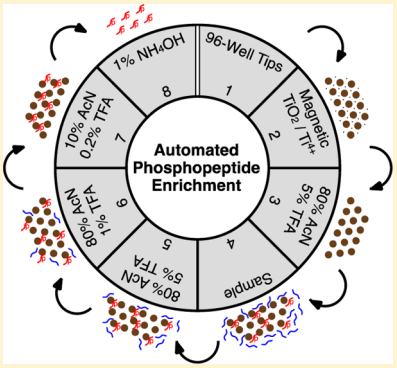

Post-translational protein phosphorylation is an important medium for cellular signal transduction.[1] Protein kinases and phosphatases are often deregulated in disease, and pharmacological modulation of phosphorylation-dependent signal transduction is an active area of research.[2] Consequently, quantitative analysis of pathological phosphoproteomes is of substantial interest to the biological research community.

Liquid chromatography coupled tandem mass spectrometry (LC-MS/MS) is a powerful technology used to characterize and quantify phosphorylated proteins. However, given the low stoichiometric abundance of phosphorylated residues within the proteome, phosphopeptide enrichment is required for comprehensive phosphoproteomic analysis. Due to the complexity and dynamic range of the phosphoproteome, sample prefractionation is commonly used to obtain comprehensive coverage.[3] Popular prefractionation techniques include strong cation exchange (SCX),[4] hydrophilic interaction liquid chromatography (HILIC),[5] and electrostatic repulsion hydrophilic interaction chromatography (ERLIC).[6] Subsequent affinity-based phosphopeptide enrichment commonly employs metal dioxides (such as titanium and zirconium) or immobilized metal ion affinity chromatography (IMAC).[7−11] Despite the established performance of these matrices, a limited number of workflows have been developed for automation.[12−14] Consequently, existing affinity enrichment methodologies still operate in either manual batch-mode or as manual prepacked spin-columns.

Extensive upstream chromatographic separation massively expands the number of samples for phosphopeptide enrichment processing. Successful approaches to avoid prefractionation have been reported for samples with limited input variables.[15,16] However, these methods do not facilitate the uniform parallel phosphopeptide enrichments required for the increased numbers of biological variables/replicates now common in phosphoproteomics. Such multivariate expansions are further exacerbated by the contemporary trend toward multisite proteomic projects.[17−19] These endeavors require interlaboratory integration of large sample sets and demand invariable sample processing across disparate users. Collectively, these factors increase both the number of simultaneous phosphopeptide enrichments required for phosphoproteomic analysis and the demand for unified sample-to-sample enrichment.

Received: July 7, 2014
Accepted: September 18, 2014
Published: September 18, 2014

Large-scale manual phosphopeptide enrichment suffers from limited throughput and may inadvertently introduce sample-to-sample enrichment bias. To address these limitations, a high-performance, easily operated, and technically uniform method for phosphopeptide enrichment is desirable.

Here, we report the application of magnetic hyper-porous polymer matrix microspheres for high-throughput, reproducible phosphopeptide enrichment. We characterize the performance of both TiO_2 and Ti-IMAC affinity matrices and describe how hyper-porous magnetic microspheres can be coupled to a magnetic particle-processing robot to facilitate automated phosphopeptide enrichment. We provide a free downloadable program so that this method can be reproduced across laboratories. The workflow employs noncustom, off-the-shelf equipment and is accessible to any laboratory interested in phosphopeptide analysis.

EXPERIMENTAL SECTION

Automated Phosphopeptide Enrichment. All experiments were performed with a KingFisher Flex (Thermo Scientific) magnetic particle-processing robot. The automated phosphopeptide enrichment program was developed using BindIt Software 3.0 (Thermo Scientific). The program file has been uploaded alongside the MS/MS data (see below) with the identifier Automated_Phosphopeptide_Enrichment.msz. This program can be freely downloaded and run on any KingFisher Flex system. TiO_2 (MR-TID010) and Ti-IMAC (MR-TIM010) hyper-porous magnetic microspheres were purchased from ReSyn Biosciences. The KingFisher Flex was configured for automated phosphopeptide enrichment, as illustrated in Figure 1a. In brief, deep-well 96-well plates (VWR 733-3004) were assigned to each of the eight carousel positions. Individual positions were loaded with (1) 96-well tip heads (Thermo Scientific); (2) hyper-porous magnetic microspheres (in 100% MeCN); (3) wash buffer 1 (80% MeCN, 5% TFA, + 1 M glycolic acid); (4) 100 μg Lys-C/trypsin digested lysate (in 80% MeCN, 5% TFA, + 1 M glycolic acid); (5) wash buffer 1; (6) wash buffer 2 (80% MeCN, 1% TFA); (7) wash buffer 3 (10% MeCN, 0.2% TFA); and (8) elution buffer (1−5% NH4OH). 500 μL of the relevant buffer was added to each well, except for the sample binding and elution steps, where only 200 μL of sample and elution buffer were used. Unless stated otherwise, all experiments were performed with the buffers described above, 1 mg of magnetic microspheres, and three automated phosphopeptide enrichment cycles. (Technical note: The amount of microspheres can greatly affect enrichment performance.[20] For maximum sample-to-sample fidelity, vortex the microsphere slurry before aliquoting.)

Following each enrichment cycle, phosphopeptides fractions were immediately acidified to 0.5% TFA/10% FA, desalted using OLIGO R3 resin[21] (Life Technologies 1-1339-03), and lyophilized. Samples were resuspended in 0.1% formic acid prior to analysis by LC-MS/MS.

Additional materials and methods can be found in the Supporting Information.

RESULTS AND DISCUSSION

Performance of Magnetic Hyper-Porous TiO_2 and Ti-IMAC Microspheres. Advances in emulsion-derived particle development have permitted the production of hyper-porous cross-linked polymeric lattices.[22] This technology has recently been used to generate metal-dioxide-bound magnetic microspheres for phosphopeptide enrichment. To evaluate the phosphopeptide enrichment performance of these matrices, TiO_2, ZrO_2, and Ti-IMAC hyper-porous magnetic microspheres (MagReSyn) were compared to established solid-bead phospho-affinity reagents (GL Science Titansphere TiO_2 and GE Healthcare MagSeph TiO_2). For each comparison, 1 mg of microspheres was combined with 500 μg of human tryptic digest, and the manufacturer's protocol was followed.

To track phosphopeptide retention, we first incubated each product with 500 μg of ^{32}P-labeled cell lysates in manual batch mode, washed and eluted. "Unbound" (remaining in the tube), "bound" (remaining on the microspheres), and "eluted" ^{32}P-containing material was quantified using a scintillation counter (Supplementary Figure 1a, Supporting Information). Elution efficiency was higher from magnetic Ti-IMAC (MagReSyn), followed by Titansphere TiO_2 (GL) and magnetic TiO_2 (MagReSyn). Both the ZrO_2 (MagReSyn) and magnetic-sepharose TiO_2 (GE) displayed poorer phosphopeptide elution. Less material was retained on the hyper-porous magnetic TiO_2, ZrO_2, and Ti-IMAC matrices following elution

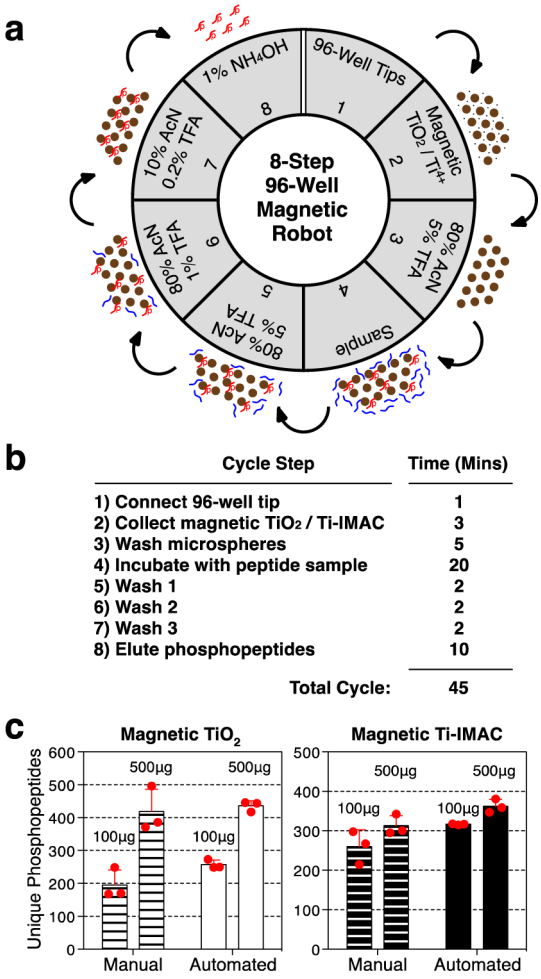

Figure 1. Robotic magnetic automated phosphopeptide enrichment. (a) KingFisher Flex configured for automated phosphopeptide enrichment. (b) Automated phosphopeptide enrichment steps (program has been deposited in PRIDE: PXD000892). (c) 100 μg and 500 μg of a common tryptic digest was phospho-enriched using TiO_2 and Ti-IMAC hyper-porous microspheres via manual and automated methods and analyzed by LC-MS/MS. DDA runs, red dots, n = 24.

dx.doi.org/10.1021/ac5025842 | Anal. Chem. 2014, 86, 10296−10302

than on the nonmagnetic TiO_2 (GL) and magnetic-sepharose TiO_2 (GE).

To investigate how this behavior translated to unique phosphopeptide identification, we repeated these experiments and analyzed eluted samples by LC-MS/MS. The highest numbers of unique phosphopeptides were identified using Ti-IMAC (MagReSyn), followed by TiO_2 (MagReSyn), ZrO_2 (MagReSyn), Titansphere TiO_2 (GL science) and MagSeph TiO_2 (GE) (Supplementary Figure 1b, Supporting Information). Unfortunately, as the total surface area and chemical composition of these reagents is proprietary, the mechanism underlying this improved performance is currently unclear. When compared to all other microspheres, Ti-IMAC (MagReSyn) and TiO_2 (MagReSyn) demonstrate a ∼15% preference for acidic residues C-terminal of the phosphorylation (Supplementary Figure 1c, Supporting Information). Conversely, TiO_2 (GL) and TiO_2 (GE) display a ∼15% bias for proline at position +1 and ∼2−5% preference for basic residues C-terminal of the phosphorylation. This data suggests the structural matrix supporting the primary enrichment chemistry influences phosphopeptide affinity. In agreement with a recent comprehensive enrichment bias study,[23] Ti-IMAC (MagReSyn) and TiO_2 (MagReSyn) display minimal phosphopeptide biases.

Given their capacity to enrich substantial numbers of high-fidelity phosphopeptides at high purity (>80%), we concluded magnetic hyper-porous Ti-IMAC and TiO_2 microspheres (MagResyn) are suitable for high-performance phosphopeptide enrichment.

Automated Phosphopeptide Enrichment. Given the high performance of magnetic TiO_2 and Ti-IMAC hyper-porous microspheres in manual batch mode, we hypothesized these reagents might be applicable to automated phosphopeptide enrichment using a magnetic particle processing robot. To investigate this, we reformatted the manual phosphopeptide enrichment protocol for automated use on the KingFisher Flex (Thermo Scientific). The KingFisher Flex contains eight positions that each hold a single deep 96-well plate. Each plate can be rotated into position under a 96-pin magnetic head via a central carousel. Once aligned, the 96-pin magnetic head drops down inside the 96-well plate to release, bind, or agitate the magnetic microspheres in solution. By repeating these steps in a user-defined sequence, the KingFisher Flex can transfer 96 magnetic microsphere samples between eight different solutions in a fast and uniform manner. We configured this platform to perform automated phosphopeptide enrichment by adding established phosphopeptide enrichment buffers to each plate and writing a program to transfer TiO_2/Ti-IMAC hyper-porous microspheres between the different plates.

Magnetic TiO_2/Ti-IMAC hyper-porous microspheres were added to one plate (position 2), Lys-C/trypsin digested samples were added in a separate plate (position 4), phosphopeptide enrichment wash buffers were dispensed into several plates (positions 3, 5, 6, and 7), and ammonia elution buffer to the final plate (position 8). We then compiled a program to collect the TiO_2/Ti-IMAC microspheres from position 2, wash the microspheres in position 3, incubate them with the tryptic digest in position 4, wash the microspheres (now containing bound phosphopeptides) in positions 5−7, elute the phosphopeptides in position 8 and return the microspheres to position 2 (Figure 1a,b). This program permits the concurrent phosphopeptide enrichment of 96 samples in 45 min. To facilitate uniform interlaboratory operation, we have deposited the automated phosphopeptide enrichment program alongside all LC-MS/MS data (PRIDE: PXD000892). This program can be freely downloaded and replicated on any KingFisher Flex system.

Automated Phosphopeptide Enrichment Optimization. As buffer composition can substantially affect enrichment performance,[24] we first trialled the automated phosphopeptide enrichment program under different binding and elution conditions. Previous studies suggest that glycolic acid (GA) added to the binding buffer can improve phosphopeptide enrichment efficiency from TiO_2.[24] However, GA is not currently used for Ti-IMAC enrichments.[25] Moreover, while low concentrations of ammonia solution (∼1% v/v) have been reported for elution of phosphopeptides from TiO_2,[21] much higher concentrations have been used for Ti-IMAC (∼5−10% v/v).[25,26] To deduce the optimal buffer conditions for automated phosphopeptide enrichment, we screened multiple ammonia solutions (1, 2.5, and 5 v/v) with or without 1 M GA across both TiO_2 and Ti-IMAC matrices (Supplementary Figure 2, Supporting Information). To ensure experiments were not limited by predicted microsphere capacity (500 μg of peptides/1 mg of microspheres), we used 20% of the recommend tryptic digest input (100 μg of peptides/1 mg of microspheres).

First, these results confirm magnetic TiO_2/Ti-IMAC hyper-porous microspheres are applicable to robotic automated phosphopeptide enrichment. This analysis also confirmed that GA improves phosphopeptide purity when using TiO_2 and revealed that GA has little influence on phosphopeptide purity when using Ti-IMAC. Moreover, increasing the ammonia concentration in the elution buffer reduces total phosphopeptide numbers with both TiO_2 and Ti-IMAC. Consequently, we opted to use 1 M GA loading buffer and 1% ammonia elution buffer (as also used in a manual method[24]) for all TiO_2 and Ti-IMAC automated phosphopeptide enrichments.

Successive Automated Phosphopeptide Enrichment Cycles. Following the completion of a single 45 min automated phosphopeptide enrichment cycle, the KingFisher Flex robot can be immediately restarted to perform an additional enrichment cycle. It has previously been shown that successive rounds of manual enrichment can increase phosphopeptide isolation.[27] We subsequently hypothesized that successive enrichment cycles influence phosphopeptide recovery using the automated platform. To investigate this, we performed successive automated phosphopeptide enrichments and independently analyzed the elution from each cycle by LC-MS/MS. To investigate the influence of increasing the amount of magnetic TiO_2 and Ti-IMAC during repeat binding, we performed this analysis with 1, 2, and 3 mg of magnetic microspheres (Supplementary Figure 3, Supporting Information).

In all experiments, the highest numbers of unique phosphopeptides were identified in the first cycle. However, successive cycles continued to enrich both cumulatively unique and nonunique phosphopeptides. Increasing the amount of magnetic microspheres also increased the total number of uniquely identified phosphopeptides. While additional DDA LC-MS/MS runs could explain the increase in cumulative peptides, repeated cycles also enrich smaller, lower charge-state phosphopeptides (Supplementary Figure 4, Supporting Information). Although successive enrichment cycles continue to enrich phosphopeptides, repeat bindings beyond two to three cycles do not increase the cumulative number of unique

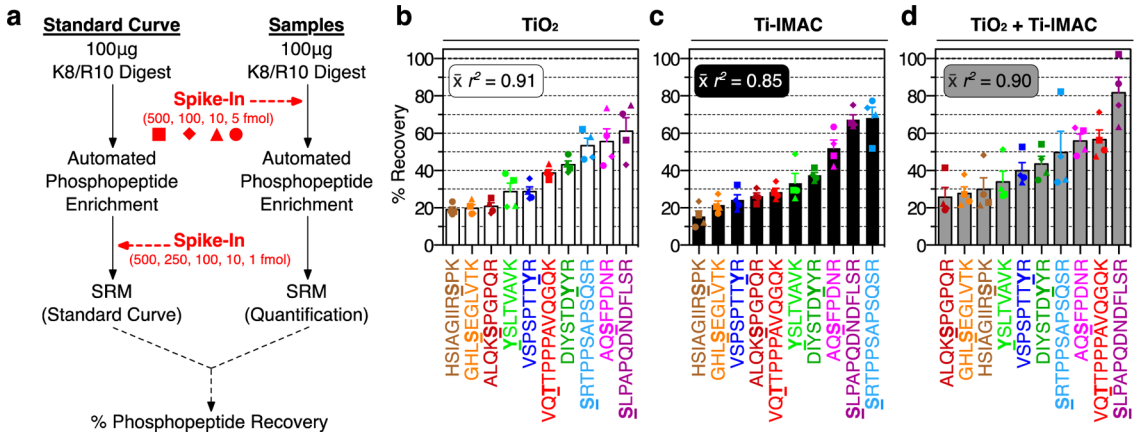

Figure 2. Automated phosphopeptide enrichment recovery. (a) Titrated synthetic phosphopeptides (n = 10) were spiked into 100 μg of heavy (K +8 Da; R +10 Da) tryptic digests either (left, standard curve) after or (right, recovery samples) before automated phosphopeptide enrichment (technical n = 3/phosphopeptide). Synthetic phosphopeptide abundance was then measured by SRM. Synthetic phosphopeptide recovery by (b) TiO_2, (c) Ti-IMAC, and (d) combined TiO_2 and Ti-IMAC automated phosphopeptide enrichment. Each dot represents the mean phosphopeptide recovery (technical n = 3) when spiked-in at 5, 10, 100, or 500 fmol. (Phosphopeptide linearity in Supplementary Table 3, Supporting Information.) LC-MS/MS SRM runs n = 51.

phosphopeptides. Phosphopeptide purity decreases with each enrichment cycle and increasing microsphere input exacerbates this deterioration. The reduction in phosphopeptide purity is particularly pronounced when using Ti-IMAC.

As the number of enrichable phosphopeptides will vary between different biological samples, we advise future users of the automated phosphopeptide enrichment protocol to validate how many cycles are required for maximum phosphopeptide enrichment of their specific samples. We concluded that one cycle of purification was suitable for most applications, and two to three cycles can be used when maximum phosphopeptide recovery is paramount.

Distinct phosphopeptide enrichment chemistries have been reported to enrich complementary segments of the phosphoproteome.[21,28,29] We subsequently hypothesized that the automated phosphopeptide enrichment platform could operate with mixed TiO_2 and Ti-IMAC microspheres. To investigate this, we performed automated phosphopeptide enrichment with titrated ratios of each microsphere matrix. Interestingly, we observed an increase in the number of unique phosphopeptides identified from a mix of TiO_2 and Ti-IMAC compared to their individual use (Supplemental Figure 5, Supporting Information). As the automated phosphopeptide enrichment platform can operate with any high-performance magnetic microspheres, this protocol can be easily adapted to employ different enrichment materials. It will be interesting to investigate alternative chemistries (as they become available) in future experiments.

Manual versus Automated Phosphopeptide Enrichment. To directly investigate how manual enrichment compared to the automated platform, we simultaneously phospho-enriched 100 and 500 μg of a consistent tryptic digest using both methods and sequentially analyzed the samples by LC-MS/MS (Figure 1c). This concurrent analysis demonstrated comparable phosphopeptide enrichment between manual and automated methods. Consequently, we concluded that the automated phospho enrichment platform performs analogous phosphopeptide identification to existing manual methodology.

Automated Phosphopeptide Enrichment Recovery. While multiple approaches for phosphopeptide enrichment are currently in use, most evaluate phosphopeptide recovery using data-dependent analysis (DDA). As such, it can be difficult to discern whether methodological improvements are due to differences in the phosphopeptide enrichment protocol or in the LC-MS/MS setup. To determine phosphopeptide recovery from the automated phosphopeptide enrichment platform, we established a targeted selected reaction monitoring (SRM) assay to robustly quantify a selection of human synthetic phosphopeptides (Supplementary Table 1 and Supplementary Figure 6, Supporting Information). To investigate the influence of phosphopeptide starting concentration, 5, 10, 100, and 500 fmol synthetic human phosphopeptides were spiked-in to a SILAC "heavy" (K +8 Da; R +10 Da) complex mouse cell-lysate tryptic digest matrix either before or after automated phosphopeptide enrichment (Figure 2a). Percentage recovery was calculated by comparing the intensity of each phosphopeptide spiked-in before automated enrichment to its standard curve derived from phosphopeptides spiked-in after enrichment (Supplementary Figure 7a, Supporting Information). Synthetic phosphopeptides were enriched with either TiO_2 (Figure 2b), Ti-IMAC (Figure 2c), or a combination of TiO_2 and Ti-IMAC (Figure 2d). Automated phosphopeptide enrichment recovered between 20 and 80% of the phosphopeptides tested with intrapeptide mean coefficient of variation (CV) of 11−46% (Supplementary Table 2, Supporting Information). All three phosphopeptide enrichment workflows demonstrated a reproducible, linear dynamic range across 2 orders of magnitude (Supplementary Figure 7b and Supplementary Table 3, Supporting Information). While this synthetic phosphopeptide portfolio is not extensive enough to extrapolate which phosphopeptide sequences are more suitable for Ti-IMAC or TiO_2 based enrichment, this data suggests some phosphopeptides are more amendable to enrichment than others. Despite this sequence-specific enrichment behavior, phosphopeptide recovery was independent of starting concentration for all phosphopeptides. Given the robust reproducibility and linearity of this assay, these synthetic phosphopeptides (Figure 2 and Supplemental Table 1, Supporting Information) also provide an accessible common standard for interlaboratory implementation of the automated phosphopeptide enrichment platform.

dx.doi.org/10.1021/ac5025842 | Anal. Chem. 2014, 86, 10296−10302

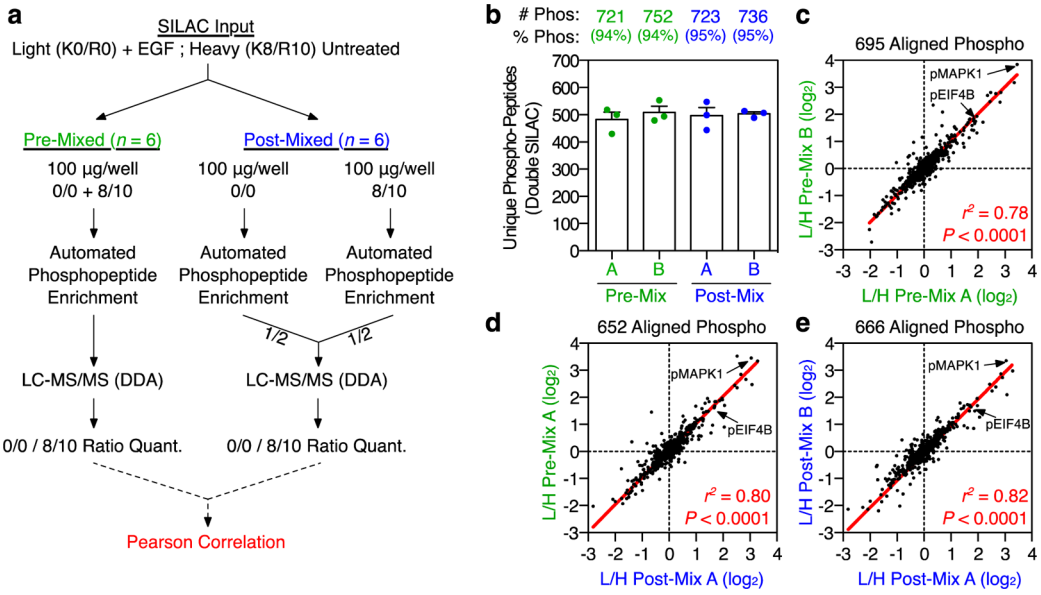

Figure 3. Automated phosphopeptide enrichment intra-plate reproducibility. (a) Light KPC cells were treated with 100 ng/mL EGF for 5 min and SILAC heavy (K +8 Da; R +10 Da) KPC cells were left untreated. Each SILAC population was digested separately and mixed either before (premixed, green) or after (postmixed, blue) automated magnetic TiO_2 phosphopeptide enrichment. Phosphopeptides were then analyzed by DDA LC-MS/MS. (b) Pre- and postmixed samples were randomly divided into two groups (A and B; n = 3/group). (c–e) The light/heavy SILAC ratios of each population were assessed by Pearson correlation (two-tailed $P < 0.0001$). LC-MS/MS DDA runs n = 12.

Automated Phosphopeptide Enrichment Intra-Plate Reproducibility. As the automated phosphopeptide enrichment platform subjects each well to identical conditions (e.g., uniform incubation times, agitation frequencies, cycles, etc.), we hypothesized this technique enriches well-to-well phosphopeptides in a highly reproducible manner. To investigate intraplate fidelity, we used the automated phosphopeptide enrichment platform to compare a "gold standard" standard SILAC experiment (samples mixed prior to enrichment)[30] with a "split" SILAC experiment (samples combined postenrichment). To this end, we compared the relative "light"/"heavy" ratios of two distinct SILAC populations mixed either before (premixed) or after (postmixed) enrichment (Figure 3a) (n = 3/group). To simulate a typical biological experiment and evaluate the dynamic range of the workflow, light labeled cells were treated with 100 ng/mL EGF for 5 min, and heavy labeled cells were left untreated. In agreement with earlier experiments, this analysis confirmed intraplate technical replicates enrich approximately equal numbers of unique phosphopeptides at high purity (>90% phosphorylated peptides) (Figure 3b). Crucially, correlating the light/heavy ratios of premixed and postmixed phosphopeptide samples showed no discernible difference in phosphopeptide enrichment fidelity between replicates ($r2$ = 0.80) (Figure 3c–e). As a result, we propose automated magnetic particle handling as a highly reproducible platform for uniform intraplate phosphopeptide enrichment.

Automated Phosphopeptide Enrichment Interplate Reproducibility. In addition to well-to-well intraplate consistency, the automated phosphopeptide enrichment program also performs identical enrichments across each individual cycle. As such, we hypothesized the automated phosphopeptide enrichment method produces high plate-to-plate enrichment reproducibility. To investigate interplate fidelity, we divided a single unlabeled tryptic digest into 5 aliquots and performed automated phosphopeptide enrichment on each aliquot across 5 consecutive days. Enrichments were conducted using TiO_2 (Figure 4a), Ti-IMAC (Figure 4b), and a mixture of TiO_2 and Ti-IMAC (Figure 4c; n = 3/condition/day). The respective MS1 precursor areas for each phosphopeptide were subsequently correlated across all 5 days. This experiment confirmed interplate replicates enrich approximately equal numbers of unique phosphopeptides at high fidelity (>90% phosphorylated peptides). Moreover, by correlating the MS1 precursor areas for each phosphopeptide across all 5 days, this analysis confirmed the automated phosphopeptide enrichment platform performs highly reproducible interplate phosphopeptide enrichment (TiO_2 $\bar{x}$ $r2$ = 0.78, Ti-IMAC $\bar{x}$ $r2$ = 0.81, TiO_2 + Ti-IMAC $\bar{x}$ $r2$ = 0.85). This high reproducibility suggests automated phosphopeptide enrichment could be applicable to accurate intraplate and interplate label-free phosphoproteomic analysis. As multiple phosphopeptide enrichments are likely to be performed over different days during a real biological project, this data also suggests phosphopeptides will be uniformly enriched across multiple experiments.

Moreover, the high interplate reproducibility suggests consistent interlaboratory exchange of data across multiple operators is possible. As a result, we propose automated magnetic particle handling as a highly robust platform for reproducible interplate phosphopeptide enrichment.

Automated Phosphopeptide Enrichment For Label-Free Quantitative Phosphoproteomics. Given the excellent reproducibility, we hypothesized that automated phosphopeptide enrichment can be used for multivariate label-free quantitative phosphoproteomics. To investigate this in a relevant biological system, we studied phosphorylation-dependent signaling of oncogenic KRAS (KRAS-G12D) in pancreatic ductal adenocarcinoma (PDA) cells. KRAS-G12D is the primary driving oncogenic mutation in PDA[31,32] and underpins aberrant cellular signaling.

Three distinct isolations of KRAS-G12D inducible cells (iKRAS)[31] were switched between KRAS-WT and KRAS-

dx.doi.org/10.1021/ac5025842 | Anal. Chem. 2014, 86, 10296–10302

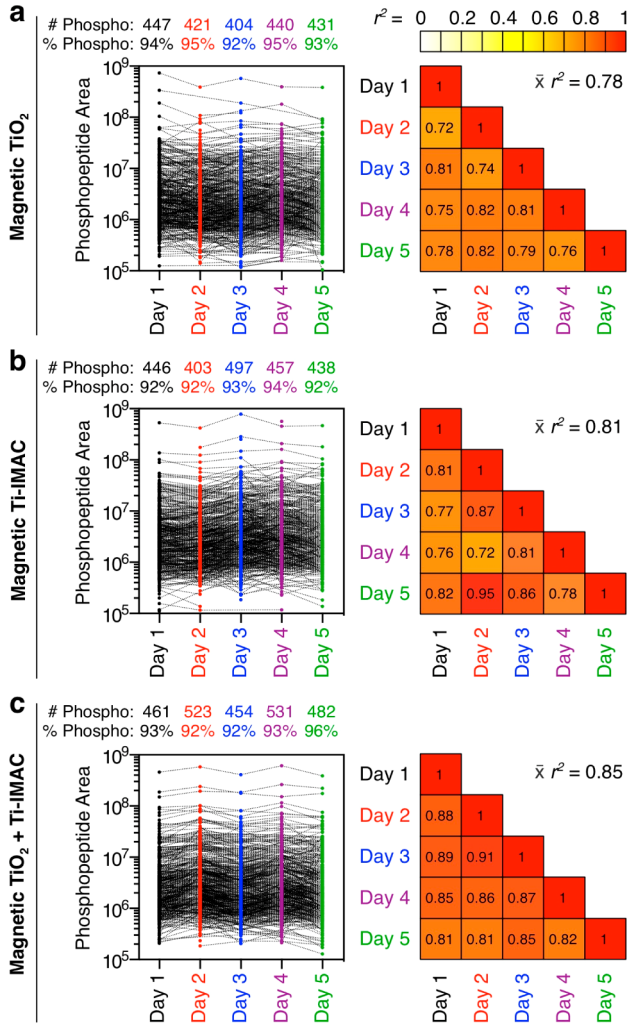

Figure 4. Automated phosphopeptide enrichment interplate reproducibility. Daily automated phosphopeptide enrichments of a common 100 μg sample of tryptic digest were performed across 5 consecutive days. Enrichments were conducted using (a) 1 mg of TiO_2, (b) 1 mg of Ti-IMAC, and (c) 1 mg of a mixture of TiO_2 and Ti-IMAC (n = 3/day). The respective precursor areas for each phosphopeptide were calculated and Pearson correlated across all 5 days. Two-tailed test for all correlations P < 0.0001. LC-MS/MS DDA runs n = 45.

G12D (via doxycycline; Supplementary Figure 8, Supporting Information) for 24 h, harvested and processed for automated phosphopeptide enrichment. Samples were prepared in biological and technical triplicate from each cell isolation (total unique phosphopeptide samples n = 54) (Figure 5a). LC-MS/MS MS1 phosphopeptide precursor area quantification revealed broad differential phospho-regulation across all three cell isolations following oncogenic KRAS induction (Supplementary Figure 9a, Supporting Information). Total phosphoproteomic phenotypes resolved oncogenic genotypes in principle component analysis (PCA) space (Figure 5b and Supplementary Figure 9b, Supporting Information). Moreover, given the high technical reproducibility of the automated phosphopeptide enrichment platform, combined with the ability to process multiple technical and biological replicates, rigorous statistical analysis of label-free phosphoproteomic data can be performed (Supplementary Figure 9c, Supporting Information). For example, significantly regulated MAPK1/3 phosphorylation was observed across all biological conditions (Figure 5c). In addition, multivariate analysis revealed phosphosites that were consistently and significantly regulated across all three distinct cell isolations (Figure 5d). By processing 54 samples across multiple cell lines and biological replicates, the automated phosphopeptide enrichment platform identified a core panel of significantly KRAS-G12D regulated phosphosites common to all PDA cells (Supplementary Table 4, Supporting Information).

Given its ability to process large numbers of distinct biological samples in a uniform manner, we propose automated phosphopeptide enrichment as a robust platform for statistical investigation of multivariate phosphoproteomic experiments.

CONCLUSIONS

As all reagents and equipment are readily available, the reported automated phosphopeptide enrichment platform can be easily implemented across multiple laboratories interested in phosphoproteomic analysis. Given the rapid (45 min), reproducible ($r2$ = 0.80) and high-fidelity (>90% phosphopeptide purity) properties of this approach, we propose automated magnetic phosphopeptide enrichment as an easily accessible method for uniform phosphopeptide enrichment.

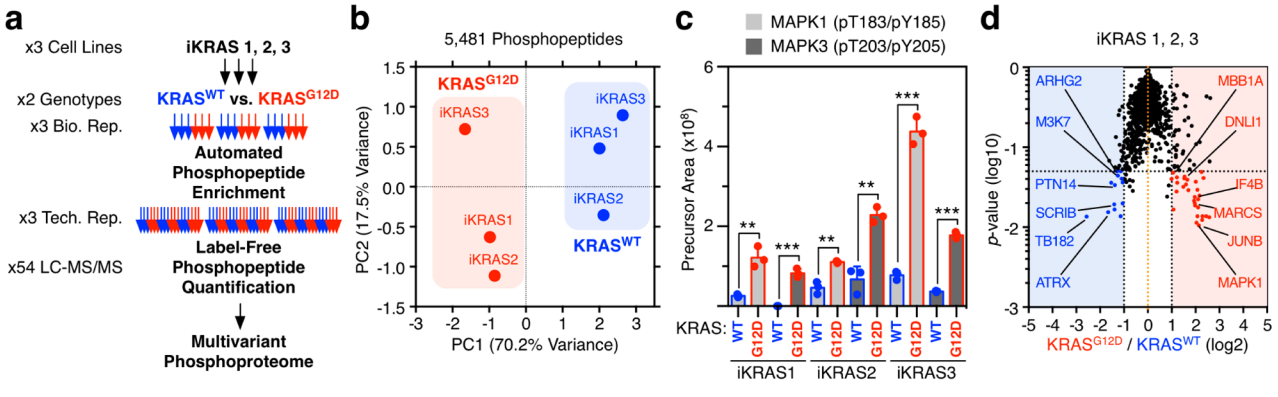

Figure 5. Multivariate sample automated phosphopeptide enrichment. (a) Experimental workflow. (b) PCA of label-free phosphoproteomic quantification resolves WT and G12D KRAS genotypes. (c) Significant phosphorylated MAPK1 (T183/Y185) and MAPK3 (T203/Y205) following oncogenic KRAS (biological replicates; two-tailed t-test; *<0.05, **<0.01, ***<0.001). (d) Significant differentially phosphorylated peptides across all three cell lines (two-tailed t-test <0.05). (Annotated data in Supplementary Table 4, Supporting Information). LC-MS/MS DDA runs n = 54.

dx.doi.org/10.1021/ac5025842 | Anal. Chem. 2014, 86, 10296−10302

■ ASSOCIATED CONTENT

Supporting Information

Additional information as noted in the text. This material is available free of charge via the Internet at http://pubs.acs.org.

■ AUTHOR INFORMATION

Corresponding Author

*E-mail: claus.jorgensen@cruk.manchester.ac.uk.

Author Contributions

C.T., J.S., and C.J. conceived the project; C.T., J.W., D.J.L., and C.J. planned experiments; C.T., J.W., R.G., and D.J.L. conducted experiments and analyzed data; J.W., J.V., K.B., M.T., and J.S. provided reagents and technical expertise; C.T. and C.J. wrote the paper; C.J. and D.A.L. oversaw the project.

Notes

The authors declare no competing financial interest.

■ ACKNOWLEDGMENTS

C.T. is funded by a Sir Henry Wellcome Postdoctoral Fellowship (098847/Z/12/Z). C.J. holds a Cancer Research UK Career Establishment Award (C37293/A12905). The authors would like to acknowledge colleagues at The ICR and the Cell Communication Team for valuable input. We would also like to acknowledge Alba Gonzalez, David Campbell, and Kenneth Beattie for their valuable input and Owen Sansom and Ronald DePinho for their generous sharing of reagents.

■ REFERENCES

(1) Pawson, T.; Scott, J. D. *Trends Biochem. Sci.* **2005**, *30* (6), 286−290.
(2) Fedorov, O.; Muller, S.; Knapp, S. *Nat. Chem. Biol.* **2010**, *6* (3), 166−169.
(3) Olsen, J. V.; Mann, M. *Mol. Cell. Proteomics* **2013**, *12* (12), 3444−3452.
(4) Beausoleil, S. A.; et al. *Proc. Natl. Acad. Sci. U.S.A.* **2004**, *101* (33), 12130−12135.
(5) McNulty, D. E.; Annan, R. S. *Mol. Cell. Proteomics* **2008**, *7* (5), 971−980.
(6) Alpert, A. J. *Anal. Chem.* **2008**, *80* (1), 62−76.
(7) Neville, D. C.; et al. *Protein Sci.* **1997**, *6* (11), 2436−2445.
(8) Ficarro, S. B.; et al. *Nat. Biotechnol.* **2002**, *20* (3), 301−305.
(9) Kuroda, I.; et al. *Anal. Sci.* **2004**, *20* (9), 1313−1319.
(10) Pinkse, M. W.; et al. *Anal. Chem.* **2004**, *76* (14), 3935−3943.
(11) Larsen, M. R.; et al. *Mol. Cell. Proteomics* **2005**, *4* (7), 873−886.
(12) Pinkse, M. W.; et al. *J. Proteome Res.* **2008**, *7* (2), 687−697.
(13) Richardson, B. M.; et al. *J. Biomol. Tech.* **2013**, *24* (1), 8−16.
(14) Ficarro, S. B.; et al. *Anal. Chem.* **2009**, *81* (11), 4566−4575.
(15) Albuquerque, C. P.; et al. *Mol. Cell. Proteomics* **2008**, *7* (7), 1389−1396.
(16) Ficarro, S. B.; et al. *Mol. Cell. Proteomics* **2011**, *10* (11), O111 011064.
(17) Paulovich, A. G.; et al. *Mol. Cell. Proteomics* **2010**, *9* (2), 242−254.
(18) Kuhn, E.; et al. *Mol. Cell. Proteomics* **2012**, *11* (6), M111 013854.
(19) Prakash, A.; et al. *J. Proteome Res.* **2012**, *11* (8), 3986−3995.
(20) Engholm-Keller, K.; et al. *J. Proteomics* **2012**, *75* (18), 5749−5761.
(21) Thingholm, T. E.; et al. *Mol. Cell. Proteomics* **2008**, *7* (4), 661−671.
(22) Jordaan, J., et al., Emulsion-Derived Particles, 2009, Patent WO2009057049.
(23) Matheron, L.; et al. *Anal. Chem.* **2014**, *86* (16), 8312−8320.
(24) Jensen, S. S.; Larsen, M. R. *Rapid Commun. Mass Spectrom.* **2007**, *21* (22), 3635−3645.
(25) Zhou, H.; et al. *Nat. Protoc.* **2013**, *8* (3), 461−480.
(26) Zhou, H.; et al. *Mol. Cell. Proteomics* **2011**, *10* (10), M110 006452.
(27) Palmisano, G.; et al. *Mol. Cell. Proteomics* **2012**, *11* (11), 1191−1202.
(28) Bodenmiller, B.; et al. *Nat. Methods* **2007**, *4* (3), 231−237.
(29) Tsai, C. F.; et al. *Anal. Chem.* **2014**, *86* (1), 685−693.
(30) Russell, M. R.; Lilley, K. S. *J. Proteomics* **2012**, *77*, 441−454.
(31) Ying, H.; et al. *Cell* **2012**, *149* (3), 656−670.
(32) Collins, M. A.; et al. *J. Clin. Invest.* **2012**, *122* (2), 639−653.